

# Ga<sub>2</sub>O<sub>3</sub> and GaN Semiconductor Hollow Spheres\*\*

Xiaoming Sun and Yadong Li\*

Both monoclinic Ga<sub>2</sub>O<sub>3</sub> and Wurtzite-structured GaN are wide-band-gap semiconductors (energy gap,  $E_g = 4.9$  eV and 3.39 eV, respectively) that exhibit luminescence and conduction properties, thus, they have potential applications in optoelectronic devices,<sup>[1–8]</sup> high-temperature stable gas sensors,<sup>[9]</sup> and high-temperature/high-power electronic devices.<sup>[10,11]</sup> The future of full-colored, flat panel displays, blue lasers, and optical communication is likely to be based on GaN.<sup>[5,12]</sup> Nanostructured Ga<sub>2</sub>O<sub>3</sub> and GaN with varied morphology, for instance, nanoparticles,<sup>[13]</sup> nanorods,<sup>[14]</sup> nanowires,<sup>[3,15]</sup> nanobelts,<sup>[4,16]</sup> and nanotubes<sup>[5–6,17–18]</sup> have been prepared. However, monodispersed spherical structures of the two semiconductor compounds have not been prepared up to now.

Monodispersed micro- or nanospheres, as a kind of competitive building blocks for future nanodevices, have become a new focus of research. This interest has arisen because it is now relatively easy to synthesize uniform spheres and to control their size, and these spheres can self-assemble into 2D or 3D colloidal arrays or photonic band gap crystals.<sup>[19–23]</sup> The preparation of uniform micro- or nanospheres of semiconducting materials would enable their use as building blocks for new photonic crystals or as model systems for light scattering, which are of both theoretical and practical significance. New approaches to semiconductor hollow spheres have been made in the last five years.<sup>[24–33]</sup> Semiconducting oxide ceramic hollow spheres (e.g., TiO<sub>2</sub>, SnO<sub>2</sub>) have been prepared by templating the sol-gel precursor solutions with monodispersed latex beads.<sup>[24]</sup> By alternating the shape and structure of the templates, the morphology of hollow structures can also be changed.<sup>[25,26]</sup> The II–VI family of semiconductor luminescent nanoparticles, such as CdTe, CdS, ZnS, have been assembled on spherical templates to form luminescent shells by using a layer-by-layer self-assembly strategy,<sup>[27–29]</sup> sonochemical deposition,<sup>[30]</sup> or chemical-bath deposition.<sup>[31–32]</sup> Very recently, our group has developed a solution-based template-free route to ZnSe semiconducting hollow spheres by condensing ZnSe nanoparticles on a liquid–gas interface.<sup>[33]</sup> Herein, we report the application

[\*] X. Sun, Prof. Dr. Y. Li  
Department of Chemistry  
The Key Laboratory of Atomic and Molecular Nanosciences  
(Ministry of Education)  
Tsinghua University  
Beijing, 100084 (China)  
Fax: (+86) 10-6278-8765  
E-mail: ydli@mail.tsinghua.edu.cn

[\*\*] This work was supported by the NSFC (20025102, 50028201, 20151001), the Foundation for the Author of National Excellent Doctoral Dissertation of P.R. China, and the State Key Project of Fundamental Research for nanomaterials and nanostructures.

of a facile surface-layer-absorption (SLA) templating technique to obtain monodispersed  $\text{Ga}_2\text{O}_3$  and GaN hollow spheres.

The strategy used to obtain monodispersed hollow  $\text{Ga}_2\text{O}_3$  and GaN spheres can be divided into three steps (Figure 1):

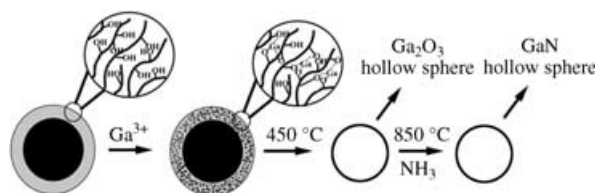


**Figure 1.** Schematic mechanism for the formation of GaN hollow spheres using carbon spheres as templates.

1) the adsorption of gallium ions from solution into surface layer; 2) calcination of the composite spheres in air to remove the carbon core, which results in oxide hollow spheres; 3) in situ conversion of the as-prepared oxide hollow spheres into nitride hollow spheres in an ammonia atmosphere at 700–900 °C. There are some essential differences between the current strategy and traditional strategies.<sup>[21–32,34,35]</sup> In traditional templating processes, which use latex or silica as templates, a coating is deposited on the sacrificial core by controlled surface precipitation/absorption of the inorganic precursors from a solution/suspension. These processes usually require alkoxides as a starting material (e.g., in sol–gel methods), or use nanoparticles as “building units” and polyelectrolytes as “glue”.<sup>[34]</sup> The core is then subsequently removed by thermal or chemical means, thus leaving behind hollow spheres.<sup>[35]</sup> During the process, surface modification is usually required for efficient adsorption and the experimental parameters must be precisely controlled to avoid heterogeneous agglomeration. In most cases, the growth is outward from the template surface,<sup>[21–25,34,35]</sup> and the void formed is approximately equal to the original size of the template. However, in our method, the templates used were carbon spheres prepared by dehydrating glucose or sucrose under hydrothermal conditions.<sup>[36]</sup> The surface of the spheres is hydrophilic and has a distribution of  $-\text{OH}$  and  $-\text{C}=\text{O}$  groups similar to that of polysaccharide in,<sup>[36]</sup> which makes surface modification unnecessary. When the carbon spheres are dispersed in solutions of metal salts, the cations are adsorbed into the surface. Agglomeration is naturally avoided because cations are absorbed into the surface layer to form a composite shell rather than form a heterogeneous coating. In the following calcination process, the metal atoms in the shell become denser, the spheres contract and cross-link to form metal-oxide hollow spheres, which are a smaller replica of the carbon spheres ( $\approx 40\%$ ). The salts (e.g., chlorides) can thus be used as the starting material instead of alkoxides, which reduces the preparation cost. The use of transition-metal salts should lead to hollow spheres of different compositions. We believe that this is a general, simple, and cheap approach to hollow spheres. Moreover, since the thickness of the functional “surface layer” is predetermined by hydrothermal synthesis, the integrity and uniformity of the

shell of final products can be ensured in this way. Herein, we demonstrate that gallium ions can be adsorbed into the surface layer and then transformed into oxide and nitride under the right conditions.

Carbon spheres were prepared according to a reported procedure.<sup>[36]</sup> A typical image obtained by scanning electronic microscopy (SEM) is shown in Figure 2a. Zeta potential analysis on the spheres indicated that the surfaces of the spheres were negatively charged in water (pH 7,  $\zeta = -47$  eV). However, this value changed to  $-18$  eV when the spheres were ultrasonicated in a solution of  $\text{GaCl}_3$  (0.5 M) for 10 min, washed (centrifugation and redispersion in water, five cycles) and suspension aged for 24 h before analysis. This result implies that  $\text{Ga}^{3+}$  ions were adsorbed into the surface layer of the carbon spheres.

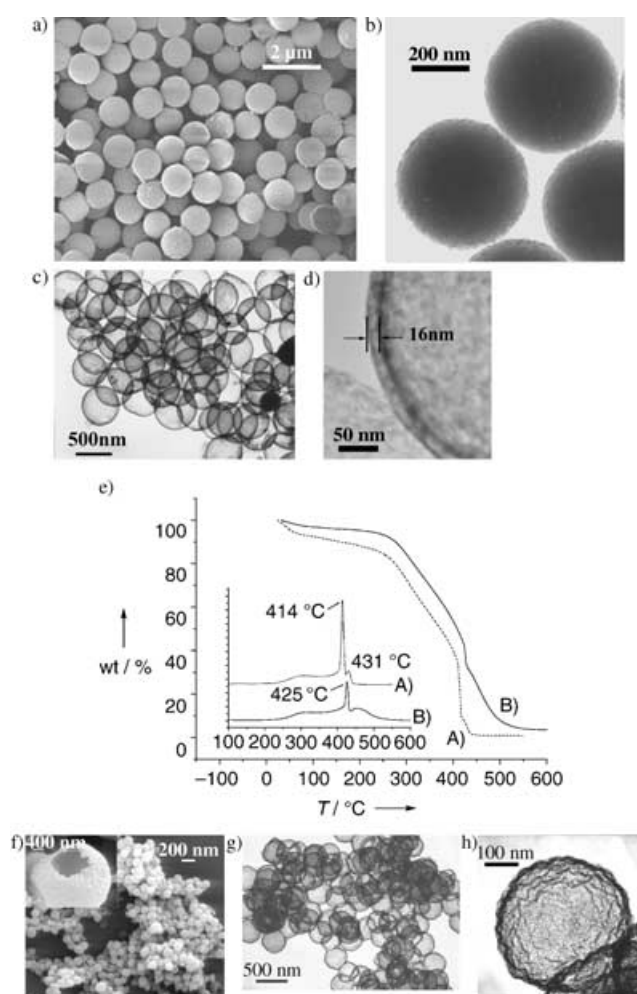


**Figure 2.** a) Typical SEM image of carbon spheres; b) typical TEM image of carbon spheres; c,d) typical TEM image of  $\text{Ga}_2\text{O}_3$  hollow spheres; e) TGA plots of A) templating carbon spheres and B) Ga-adsorbed carbon spheres (inset: their differential curves); f) SEM image of intact  $\text{Ga}_2\text{O}_3$  hollow spheres 100 nm in diameter (inset: SEM image of large hollow spheres 1500 nm in diameter, which were deliberately broken by crushing in a mortar to show the hollow interior); g,h) typical TEM images of  $\text{Ga}_2\text{O}_3$  hollow spheres prepared by using templating carbon spheres from sucrose rather than glucose solutions.

Images of the spheres obtained by transmission electron microscopy (TEM) indicate that the gallium ions were adsorbed into the surface layer rather than grafted onto the surface (Figure 2b). No amorphous layer or aggregations of gallium compounds, such as hydroxides, were observed, though energy dispersive X-ray (EDX) analysis on the spheres clearly revealed the existence of elemental Ga and an atomic ratio of Ga to Cl greater than 10:1. This result indicates that cationic  $\text{Ga}^{3+}$  ions were selectively adsorbed in the surface layer and anionic  $\text{Cl}^-$  ions were excluded since the ratio of  $\text{Ga}^{3+}$  to  $\text{Cl}^-$  in bulk solution was 1:3, while that of adsorbed ions was greater than 10:1 after washing cycles. We propose that the polysaccharide-like layer at the surface of carbon spheres serves as an adsorbent, which can chelate  $\text{Ga}^{3+}$  ions and protect them from heterogeneous coagulation or being washed off. It is noteworthy that the size of carbon spheres can be manipulated in the range from 200 nm to 4000 nm, or even larger, by adjusting experimental parameters. Smaller spheres (about 400 nm in diameter) were chosen to show the surface morphology more clearly.

The gallium-adsorbed carbon spheres were calcined in air to remove the carbon component, resulting in  $\text{Ga}_2\text{O}_3$  hollow spheres. TEM micrographs reveal the hollow structure of the calcined samples (Figure 2c). A selected-area electron-diffraction pattern shows that the spheres are polycrystalline. XRD characterization indicates that the as-prepared sample is  $\text{Ga}_2\text{O}_3$  (JCPDS 060509, shown in Figure 3a). The average crystalline size was about 4 nm, as calculated from the broad peaks by using the Scherrer equation. The hollow spheres prepared from carbon spheres of  $1000 \pm 50$  nm in diameter (shown in Figure 2a) had diameters of  $370 \pm 20$  nm, about 60% smaller than the starting spheres and had a shell thickness of about 16 nm as measured by using a TEM image that had been further magnified (Figure 2d). The large shrinkage ratio is essentially different to that obtained by using traditional sacrificial-core methods. In these methods, the prepared hollow spheres were nearly the same size or slightly smaller than the template.<sup>[21–26,34,35]</sup> We believe that the large shrinkage is caused by further dehydration of the loosely cross-linked structure of the carbon spheres, which leads to densification of  $\text{Ga}^{3+}$  ions in surface layer. Consequently, cross-linking and crystallization of gallium oxide take place when the carbon is removed in air during the calcination process, thus resulting in metal-oxide hollow spheres.

This hypothesis was partly evidenced by thermal gravimetric analysis (TGA) of Ga-loaded templates and templating carbon spheres. The similarity of the two curves (shown in Figure 2e) revealed that the two microspheres experience similar oxidation procedures: first ( $< 400^\circ\text{C}$ ), a slow loss of weight attributed to the further dehydration and densification of carbon spheres; second, sharp weight-loss peak at 414 or  $425^\circ\text{C}$  (Figure 2e, inset), which are attributed to burning of the carbon spheres. The weight-loss peak from the Ga-adsorbed spheres shifts to a higher temperature; it is considered that Ga absorption might inhibit the inner oxidation. After the sharp weight loss, there is still a process of weight loss ( $430\text{--}550^\circ\text{C}$ ), which might be caused by oxidation of carbon found deep within the core. The final weight of Ga-adsorbed spheres was measured to be 3.3%.

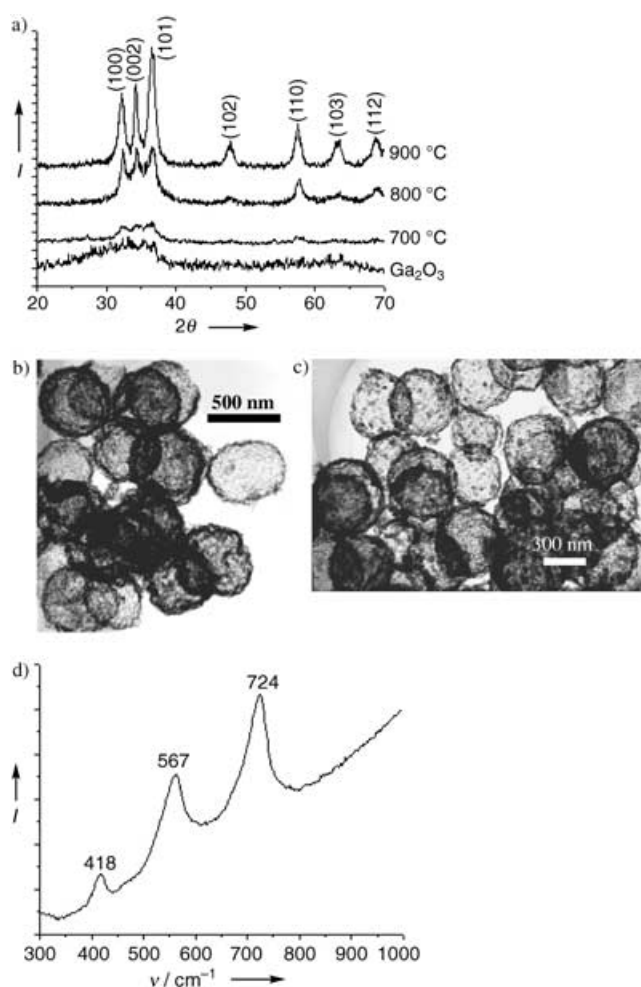


**Figure 3.** a) XRD patterns of  $\text{Ga}_2\text{O}_3$  and GaN hollow spheres prepared at  $700^\circ\text{C}$ ,  $800^\circ\text{C}$ , and  $900^\circ\text{C}$ ; b,c) typical TEM image of GaN hollow spheres prepared at  $700^\circ\text{C}$  and  $900^\circ\text{C}$ , respectively. d) Raman spectrum of GaN hollow spheres prepared at  $900^\circ\text{C}$ .  $I$  = intensity, arbitrary units.

By alternating the size of templates from 200 nm to 4  $\mu\text{m}$ , the average size of hollow spheres can be manipulated in the range from 100 nm to 1.5  $\mu\text{m}$  with an almost constant shrinkage ratio about 40%. Figure 2f and the inset show the SEM of some intact and individual broken hollow spheres with diameters of  $100 \pm 5$  nm and 1500 nm, respectively. Though the diameter of the hollow spheres may vary considerably, the thickness of the shell changes little (16 nm) even when the concentration of  $\text{GaCl}_3$  is reduced from 0.5 M to 0.1 M or the adsorption temperature is increased from room temperature to  $90^\circ\text{C}$ . However, when the templating carbon spheres ( $1000 \pm 50$  nm) were prepared from sucrose rather than glucose solution, the hollow  $\text{Ga}_2\text{O}_3$  spheres had a rippled thinner shell ( $\approx 10$  nm) and particle size  $330 \pm 15$  nm were fabricated (Figure 2g, h). Such effects are attributed to the predetermined thickness of the “reactive-surface layer” of the carbon spheres. During the hydrothermal synthesis, there is a “growing layer” surrounding the carbon spheres, which moves outward as the size of the carbon spheres increases. As the growth process is stopped by

terminating the hydrothermal treatment, the growing layer solidifies at the surface of carbon spheres and serves as a reactive-surface layer for the adsorption of cations. The thickness of the growing layer and the subsequent reactive-surface layer should remain unchanged despite the diameters of the carbon spheres increasing with increasing hydrothermal time. When sucrose rather than glucose was used for preparation of carbon spheres, the thickness of growing layer changed, resulting in different shell structures. This synthetic aspect is also different from previous inorganic-coating sacrificial-core methods, in which the relative ratios of the reactants (e.g., alkoxide, organic solvent, and water) in the sol-gel coating process considerably influence the quality and thickness of the coating.<sup>[34]</sup> The structure of the spheres would make it a promising material for catalysis and light advanced ceramic materials.

When the  $\text{Ga}_2\text{O}_3$  hollow spheres were heated in an ammonia atmosphere at  $700^\circ\text{C}$ , GaN hollow spheres were formed. The wide-angle XRD patterns shown in Figure 3 clearly indicate the presence of the wurtzite structure of GaN (JCPDS 760703, space group P6mc). Lattice parameters calculated from the patterns ( $a = 3.191(1)$ , and  $c = 5.187(6) \text{ \AA}$ ), agree well with the standard data ( $a = 3.190$ , and  $c = 5.189 \text{ \AA}$ ). The crystallinity of final products obtained at  $700$ ,  $800$ , and  $900^\circ\text{C}$  were compared through XRD characterization (Figure 3a). The average crystalline sizes of samples obtained at these temperatures were  $4 \text{ nm}$  ( $700^\circ\text{C}$ ),  $7 \text{ nm}$  ( $800^\circ\text{C}$ ), and  $14 \text{ nm}$  ( $900^\circ\text{C}$ ), according to the Scherrer equation. These results indicate that the GaN nanoparticles recrystallize and grow at a high temperature. Figures 3b, c show the TEM images of the samples obtained at  $700^\circ\text{C}$  and  $900^\circ\text{C}$ , respectively. The shell of the former was uniform, whereas the latter was decorated randomly with nanoparticles of  $20 \text{ nm}$  in diameter. The room-temperature Raman spectrum of the hollow spheres (Figure 3d) shows three broad symmetric peaks at  $418$ ,  $567$ , and  $724 \text{ cm}^{-1}$ . The second and third peaks were assigned to first-order phonon frequencies of  $\text{E}_2(\text{high})$  and  $\text{A}_1(\text{LO})$  modes, which have been measured at  $570$  and  $730 \text{ cm}^{-1}$  for GaN nanorods.<sup>[7]</sup> The lower-frequency shift of the  $\text{E}_2(\text{high})$  peak implies that the spheres experience some strain in structure since the shift is significantly influenced by compressive or tensile strains.<sup>[37–38]</sup> The peak positioned at  $418 \text{ cm}^{-1}$  is close to an acoustic overtone peak found in the spectrum of a wurtzite GaN crystal.<sup>[39]</sup>

The tunable size range of GaN hollow spheres from  $100 \text{ nm}$  to  $1.5 \text{ }\mu\text{m}$  is especially attractive for optical applications because this range covers the band gaps in the spectral regime from the ultraviolet ( $100\text{--}400 \text{ nm}$ ), visible ( $400\text{--}800 \text{ nm}$ ), to near infrared ( $800\text{--}1500 \text{ nm}$ ), while the intrinsic emission band of GaN is also in this range ( $370 \text{ nm}$ ). Former studies indicate that the emission properties of semiconductor nanoparticles are affected by the way in which they pack and embed into the voids of the colloidal crystals.<sup>[40,41]</sup> Hollow GaN spheres with average outside diameter of  $370 \text{ nm}$  (shown in Figure 3c) were chosen for photoluminescence study since they were expected to show specific interaction with the emission of GaN. One can see that the GaN hollow spheres showed two major emission bands (Figure 4a): one centered at  $371 \text{ nm}$  and the other comprising several emissions

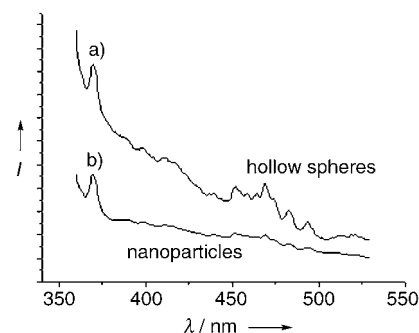


**Figure 4.** The photoluminescence spectrum of a) GaN hollow spheres and b) GaN nanoparticles.

positioned at  $452$ ,  $470$ ,  $475$ ,  $483$ , and  $494 \text{ nm}$ . The band at  $371 \text{ nm}$  is related to band-edge emission, which could be attributed to the recombination of excitons bound at neutral donor sites.<sup>[9,42]</sup> But the latter is difficult to identify.<sup>[42–45]</sup> The band positioned between the yellow luminescence ( $2.2 \text{ eV}$ ,  $563 \text{ nm}$ ) caused by deeply trap states<sup>[43,18]</sup> and the donor-acceptor pair emission ( $3.2 \text{ eV}$ ,  $380 \text{ nm}$ )<sup>[44]</sup> may be caused by impurities.<sup>[44–45]</sup> When the used reagent ( $\text{GaCl}_3$ ) was directly precipitated from solution with ammonia, dehydrated in air, and converted to GaN in  $\text{NH}_3$  at  $900^\circ\text{C}$ , the as-formed GaN nanoparticles exhibited only band-edge photoluminescence (Figure 4b). So the emission around  $470 \text{ nm}$  may be morphologically related. The shell of hollow spheres is composed of GaN nanoparticles, while the structure of GaN quantum dots at the electronic level has not yet been clearly determined,<sup>[42]</sup> which further complicates the assignment of the observed peaks to specific transitions at the present time. Further detailed optical studies, such as absorbance, reflectance, and photoluminescence, on GaN hollow spheres with different sizes and crystallinities will be reported elsewhere.

In summary, size-tunable  $\text{Ga}_2\text{O}_3$  and GaN semiconductor hollow spheres with uniform shells were prepared by using carbon spheres as templates. The size of the hollow spheres could be adjusted in the range from  $100 \text{ nm}$  to  $1.5 \text{ }\mu\text{m}$  by selecting different sized templating carbon spheres. This approach provides a general, simple, and cheap method to uniform hollow spheres. Surface modification and agglomeration is naturally avoided. Hollow spheres of other metal oxides may be prepared by using this method.

### Experimental Section

**Carbon template spheres:** In a typical procedure, glucose or sucrose ( $4\text{--}8 \text{ g}$ , analytic purity, Beijing Chemical Reagent Factory) was dissolved in water ( $40 \text{ mL}$ ) to form a clear solution. The solution was then sealed in a  $40 \text{ mL}$  teflon-lined autoclave and maintained at  $160\text{--}180^\circ\text{C}$  for  $4\text{--}20 \text{ h}$ . The black or puce products were isolated after centrifugation at  $5000 \text{ rpm}$  for  $20 \text{ min}$ . The products were centrifuged, washed, and redispersed in water, and this cycle was repeated five times. Next, the products were centrifuged, washed, and redispersed in alcohol, and this cycle was repeated five times. The spheres were then oven-dried at  $80^\circ\text{C}$  for  $4\text{--}8 \text{ h}$ .<sup>[36]</sup>

**GaN spheres:** The as-prepared carbon spheres were washed, redispersed in  $0.5 \text{ M}$   $\text{GaCl}_3$  solution, and ultrasonicated for  $10 \text{ minutes}$ . The resulting suspension was aged for  $12 \text{ h}$  before being subjected to

five cycles of centrifugation/wash/redispersion in water. The oven-dried sample was heated to 450°C in a tube furnace in air and maintained at the temperature for one hour. Ammonia (>99.5%, 30 sccm) was introduced and the temperature to 800°C at a rate of 3°C per minute. Argon was flowed into the reaction vessel at a rate of 200 sccm while maintaining the temperature at 800°C for 3 h. Slightly yellow powders were obtained as the sample was allowed to cool to room temperature. Products were characterized with XRD (Bruker D8 advance), TEM (Hitachi H800, Jeol 2010F, both operated at 200 kV), and SEM (Leo-1530). Fluorescent spectra were recorded with a Hitachi F-4500 fluorescence spectrophotometer. The quantity of Ga adsorbed onto the carbon spheres were determined by thermal gravimetric analysis (TA instruments, TGA2050) in air at a heating rate of 10°C min<sup>-1</sup> from room temperature to 600°C.

Received: October 31, 2003

Revised: April 1, 2004 [Z53212]

**Keywords:** gallium · microspheres · nanostructures · semiconductors · template synthesis

- [1] T. Harwig, F. Kellendonk, *J. Solid State Chem.* **1978**, *24*, 255–263.
- [2] L. Dai, X. L. Chen, X. N. Zhang, A. Z. Jin, T. Zhou, B. Q. Hu, Z. Zhang, *J. Appl. Phys.* **2002**, *92*, 1062.
- [3] B. Cheng, E. T. Samulski, *J. Mater. Chem.* **2001**, *11*, 2901–2902.
- [4] S. Shama, M. K. Sunkara, *J. Am. Chem. Soc.* **2002**, *124*, 12288.
- [5] F. A. Ponce, D. P. Bour, *Nature* **1997**, *386*, 351.
- [6] T. Someya, R. Werner, A. Forchel, M. Catalano, R. Cingolani, Y. Arakawa, *Science* **1999**, *285*, 1905.
- [7] S. Y. Bae, H. W. Seo, J. Park, H. Yang, H. Kim, S. Kim, *Appl. Phys. Lett.* **2003**, *82*, 4564.
- [8] C. H. Liang, G. W. Meng, G. Z. Wang, Y. W. Wang, L. D. Zhang, S. Y. Zhang, *Appl. Phys. Lett.* **2001**, *78*, 3202.
- [9] Y. X. Li, A. Trinchì, W. Włodarski, K. Galatsis, K. Kalantar-zadeh, *Sens. Actuators B* **2003**, *93*, 431.
- [10] G. Fasol, *Science* **1996**, *272*, 1751.
- [11] H. M. Kim, T. W. Kang, K. S. Chung, *Adv. Mater.* **2003**, *15*, 567.
- [12] S. Nakamura, *Science* **1998**, *281*, 956.
- [13] C. H. Wallace, S. H. Kim, G. A. Rose, L. Rao, J. R. Heath, M. Nicol, and R. B. Kaner, *Appl. Phys. Lett.* **1998**, *72*, 596–598.
- [14] W. Q. Han, S. S. Fan, Q. Q. Li, Y. D. Hu, *Science* **1997**, *277*, 1287.
- [15] X. F. Duan, C. M. Lieber, *J. Am. Chem. Soc.* **2000**, *122*, 188–189.
- [16] S. Y. Bae, H. W. Seo, J. Park, H. Yang, J. C. Park, S. Y. Lee, *Appl. Phys. Lett.* **2002**, *81*, 126–128.
- [17] J. Goldberger, R. R. He, Y. F. Zhang, S. K. Lee, H. Q. Yan, H.-J. Choi, P. D. Yang, *Nature* **2003**, *422*, 599.
- [18] J. Q. Hu, Y. Bando, D. Golberg, Q. L. Liu, *Angew. Chem.* **2003**, *115*, 3617–3621; *Angew. Chem. Int. Ed.* **2003**, *42*, 3493–3497.
- [19] Y. N. Xia, B. Gates, Y. D. Yin, Y. Lu, *Adv. Mater.* **2000**, *12*, 693–713.
- [20] W. Schärfl, *Adv. Mater.* **2000**, *12*, 1899–1908.
- [21] F. Caruso, *Top. Curr. Chem.* **2003**, *227*, 145–168, and references therein.
- [22] Y. N. Xia, B. Gates, Z. Y. Li, *Adv. Mater.* **2001**, *13*, 409, and references therein.
- [23] H. Fudouzi, Y. N. Xia, *Adv. Mater.* **2003**, *15*, 892.
- [24] Z. Y. Zhong, Y. D. Yin, B. Gates, Y. N. Xia, *Adv. Mater.* **2002**, *14*, 206–209.
- [25] Y. Lu, Y. D. Yin, Y. N. Xia, *Adv. Mater.* **2001**, *13*, 267–271.
- [26] Z. Z. Yang, Z. W. Niu, Y. F. Lu, Z. B. Hu, C. C. Han, *Angew. Chem.* **2003**, *115*, 1987–1989; *Angew. Chem. Int. Ed.* **2003**, *42*, 1943.
- [27] A. Rogach, A. Susha, F. Caruso, G. Sukhorukov, A. Kornowski, S. Kershaw, M. Möhwal, A. Eychmüller, H. Weller, *Adv. Mater.* **2000**, *12*, 333–337.
- [28] I. L. Radtchenko, G. B. Sukhorukov, N. Gaponik, A. Kornowski, A. L. Rogach, H. Möhwal, *Adv. Mater.* **2001**, *13*, 1684–1687.
- [29] D. Y. Wang, A. L. Rogach, F. Caruso, *Chem. Mater.* **2003**, *15*, 2724.
- [30] M. L. Breen, A. D. Dingsmore, R. H. Pink, S. B. Qadri, and B. R. Ratna, *Langmuir* **2001**, *17*, 903–907.
- [31] C. X. Song, G. H. Gu, Y. S. Lin, H. Wang, Y. Guo, X. Fu, Z. S. Hu, *Mater. Res. Bull.* **2003**, *38*, 917–924.
- [32] K. P. Velikov, A. van Blaaderen, *Langmuir* **2001**, *17*, 4779–4786.
- [33] Q. Peng, Y. J. Dong, Y. D. Li, *Angew. Chem.* **2003**, *115*, 3135–3138; *Angew. Chem. Int. Ed.* **2003**, *42*, 3027–3030.
- [34] F. Caruso, *Chem. Eur. J.* **2000**, *6*, 413–419.
- [35] Y. D. Yin, Y. Lu, B. Gates, Y. N. Xia, *Chem. Mater.* **2001**, *13*, 1146.
- [36] X. M. Sun, Y. D. Li, *Angew. Chem.* **2004**, *116*, 607–611; *Angew. Chem. Int. Ed.* **2004**, *43*, 597–601.
- [37] H. W. Seo, S. Y. Bae, J. Park, H. Yang, K. S. Park, S. Kim, *J. Chem. Phys.* **2002**, *116*, 9492.
- [38] M. Klose, N. Wieser, G. C. Rohr, R. Dassow, F. Scholz, J. Off, *J. Cryst. Growth* **1998**, *189/190*, 634.
- [39] C.-C. Chen, C.-C. Yeh, C.-H. Chen, M.-Y. Yu, H.-L. Liu, J.-J. Wu, K.-H. Chen, L.-C. Chen, J.-Y. Peng, Y.-F. Chen, *J. Am. Chem. Soc.* **2001**, *123*, 2791.
- [40] A. S. Susha, F. Caruso, A. L. Rogach, G. B. Sukhorukov, A. Kornowski, H. Möhwal, M. Giersig, A. Eychmüller, H. Weller, *Colloids Surf. A* **2000**, *163*, 39.
- [41] Y. A. Vlasov, K. Luterova, I. Pelant, B. N. Hönerlage, V. N. Astratov, *Appl. Phys. Lett.* **1997**, *71*, 1616.
- [42] O. I. Mičić, S. P. Ahrenkiel, D. Bertram, and A. J. Nozik, *Appl. Phys. Lett.* **1999**, *75*, 478–480.
- [43] E. R. Glaser, T. A. Kennedy, K. Doverspike, L. B. Rowland, D. K. Gaskill, J. A. Freitas, Jr., M. Asif Khan, J. N. Kuzina, D. K. Wickenden, *Phys. Rev. B* **1995**, *51*, 13326.
- [44] J. Y. Leem, C. R. Lee, J. I. Lee, S. K. Noh, Y. S. Kwon, Y. H. Ryu, S. J. Son, *J. Cryst. Growth* **1998**, *193*, 491–495.
- [45] H. J. Lozykowski, W. M. Jadwisieniczak, I. Brown, *Appl. Phys. Lett.* **1999**, *74*, 1129.